Biosensors and Bioelectronics 35 (2012) 470–474

Contents lists available at SciVerse ScienceDirect

Biosensors and Bioelectronics

journal homepage: www.elsevier.com/locate/bios

Short communication

Highly stable electrochemical immunosensor for carcinoembryonic antigen

Xiaobin Sun, Zhanfang Ma *

Department of Chemistry, Capital Normal University, Beijing 100048, China

ARTICLE INFO

Article history:
Received 9 December 2011
Received in revised form 25 February 2012
Accepted 28 February 2012
Available online 7 March 2012

Keywords:
Carcinoembryonic antigen
Electrochemical immunosensor
Gold nanoparticles
C—Au bond

ABSTRACT

The long-term stability of sensing interfaces is an important issue in biosensor fabrication. A novel stable gold nanoparticle (AuNP)-modified glassy carbon (GC) electrode interface (GC-Ph-AuNP)-based biosensor for detecting carcinoembryonic antigen (CEA) was developed. GC electrodes were modified with 1,4-phenylenediamine to form a stable layer, and then AuNPs were bound onto the GC electrodes through C—Au bonds. Anti-CEA was directly adsorbed on AuNPs fixed on the GC electrode. The linear range of the immunosensor was from 10 fg to 100 ng mL^{-1} with a detection limit of 3 fg mL^{-1} (S/N = 3). The current of the immunosensor was increased by 4% after one month. The GC-Ph-AuNP immunosensor showed high sensitivity, a wide linear range, low detection limit, and good selectivity and stability. The immobilization method of the immunosensor could be widely applied to construct other immunosensors.

1. Introduction

The precise and sensitive determination of disease-related proteins is very important in clinical diagnosis, biomedical exploit and biochemistry research (Lefkowitz et al., 2010; Dutsch-Wicherek, 2010). In particular, the clinical measurement of tumor- and infectious disease-related proteins is of great importance for early disease detection and highly reliable diagnosis (Gunaseelan et al., 2010; Coyle and Johnston, 2010). Immunoassays, as a promising approach for selective and sensitive analysis, have recently gained increasing attention in the quantitative detection of tumor markers and cancer screening (Gas et al., 2010; Bosker and Huestis, 2009). A number of immunoassay methods including chemiluminescence-, fluorescence-, Raman spectroscopy-, electrochemistry- and surface plasmon resonance-based immunoassays have been developed to determine the presence of tumor markers (Xu et al., 2011; Tang et al., 2010; Song et al., 2009; Chen et al., 2009; Bi et al., 2009; Dai et al., 2011). Electrochemical immunoassays in particular have attracted extensive interest because of advantages such as high sensitivity, a relatively low detection limit, and rapid analysis (Wang et al., 2004a,b; Centi et al., 2007; Zhang et al., 2010; Malhotra et al., 2010).

Nanobiotechnology has been widely applied in immunosensors in place of conventional sensing technologies, which has led to improvements in sensitivity, selectivity, and multiplexing capacity (Ma et al., 2002; Wang et al., 2007; Li et al., 2006). Recently, a series of gold nanomaterials suitable for immobilization of biomolecules was reported (Liu et al., 2006; Wang et al., 2006a,b; Wang et al., 2008). Gold nanoparticles (AuNPs) have received considerable attention in analytical electrochemistry because of their unique physicochemical characteristics. Especially AuNPs, have received considerable attention in analytical electrochemistry due to their particular physicochemical characteristics. Based on favorable microenvironment, large specific surface area, good biocompatibility and high conductivities between biomolecules and electrode surface, AuNPs have been used for fabrication of biosensor with enhanced analytical performance as the immobilization interface (Ma and Sui, 2002; Shi and Ma, 2011; Xu et al., 2010; Su and Mao, 2006). The long-term stability of immobilization interfaces based on AuNPs is an important issue for their application. Various strategies such as electrostatic interactions, block copolymer matrices, and chemical bonding (S—Au and NH—Au bonds) have been used to fabricate immobilization interfaces based on AuNPs (Wang et al., 2003; Xu et al., 2007; Haryono and Binder, 2006; Shenhar et al., 2005; Pacifico et al., 2005; Tognarelli et al., 2005; Yamanoi et al., 2004). However, these methods possess certain disadvantages including poor adhesion to substrates (block copolymer matrices, S—Au and NH—Au bonds), instability in certain chemical environments (electrostatic interactions and block copolymer matrices), uncontrolled growth (S—Au and NH—Au bonds and block copolymer matrices), and slow growth (electrostatic interactions (Wohltjen and Snow, 1998; Leibowitz et al., 1999; Templeton et al., 2000).

In this work, a novel immunosensor containing a stable AuNP-modified glassy carbon (GC) electrode interface (GC-Ph-AuNP) was developed to detect carcinoembryonic antigen (CEA). The immunosensor is simple, and exhibits a wide linear range (10 pg to 100 ng mL^{-1}), and a low limit of detection (LOD) of 3 fg mL^{-1} (S/N = 3).

* Corresponding author.
E-mail address: mazhanfang@yahoo.com (Z. Ma).

0956-5663/$ – see front matter © 2012 Elsevier B.V. All rights reserved.
doi:10.1016/j.bios.2012.02.061

2. Experimental

2.1. Materials

CEA was purchased from Beijing Biosynthesis Biotechnology Co. Ltd. (Beijing, China). Hydrogen tetrachloroaurate (III) hydrate ($HAuCl_4{\cdot}XH_2O$), D-(+)-glucose, ascorbic acid (AA) was achieved from Alfa Aesar (Tianjin, China). Human immunoglobulin G (IgG) was purchased Chengwen Biological Company (Beijing, China). Trisodium citrate, NaH_2PO_4, Na_2HPO_4, KCl, albumin from bovine serum (BSA), potassium ferricyanide ($K_3Fe(CN)_6$), potassium ferrocyanide ($K_4Fe(CN)_6$), 1,4-phenylenediamine (H_2N-Ph-NH_2), Sodium nitrite ($NaNO_2$), acetonitrile (CH_3CN) and HCl were obtained from Beijing Chemical Reagents Company (Beijing, China). All the reagents were of analytical grade and were used without further purification.

2.2. Apparatus

In all the procedures, the water used was purified through an Olst ultrapure K8 apparatus (Olst, Ltd., resistivity >18 MΩ). Transmission electron microscopy (TEM) was performed with a JEOL-100CX electron microscope under 80 kV accelerating voltage. Atomic-force microscopy (AFM) image were obtained in tapping mode (SPM; Vecco, USA). All electrochemical measurements were performed with a CHI-832 electrochemical analyzer (Chenhua, Shanghai, China) and a conventional three-electrode system. The working electrode was GC electrode prepared from rods with 3 mm diameter encased in epoxy resin. Platinum foil and Ag/AgCl (saturated KCl) electrode were used as the counter and reference electrodes, respectively. All potentials are reported against the Ag/AgCl reference electrode at room temperature. All differential pulse voltammetry (DPV) measurements were carried out in 0.1 M phosphate-buffer saline (pH 7.0) containing 5 mM $[Fe(CN)_6]^{4-/3-}$(PBS-$[Fe(CN)_6]^{4-/3-}$).

GC working electrodes were polished successively in 1.0, 0.3, and 0.05 μm alumina slurries. The electrodes were thoroughly rinsed with pure water and sonicated in pure water for 5 min between polishing steps. Before modification, the electrodes were dried with nitrogen gas.

2.3. Preparation of AuNPs

The AuNPs with the sizes of 5, 10, 15, 20, 40 and 65 nm were prepared according to a literature (Frens, 1973) with slight modifications. 5 nm AuNPs were prepared at room temperature by adding 1 mL 1% sodium citrate solution to the 100 mL 0.01% $HAuCl_4$ solution with stirring. After 1 min, 1.6 mL 0.075% $NaBH_4$ (dissolved in 1% sodium citrate solution) was added. The mixture was not stopped stirring until its color turned red. For 10 nm AuNPs, the preparing procedures were the same as that of 5 nm except 1 mL $NaBH_4$ solution was added. For 15, 20, 40 and 65 nm AuNPs, they were obtained by adding 5, 4, 2 and 1 mL 1% sodium citrate solution, respectively, 100 mL 0.01% boiling $HAuCl_4$ solution with vigorous stirring. The color changed from pale to blue, then to burgundy. Boiling was continued for 15 min and then stirring until the sample had cooled to room temperature.

2.4. Preparation of anti-CEA functionalized electrodes

H_2N-Ph-NH_2 (1 mM) was dissolved in 0.5 M HCl solution, and then $NaNO_2$ (1 mM) was added to the electrochemical cell. The mixture was degassed with nitrogen and then left to react for about 15 min at 0 °C. The GC electrode was cycled using cyclic voltammetry (CV) between 0.6 and −1.0 V *versus* Ag/AgCl for five cycles at a scan rate of 100 mV s^{-1} in the electrochemical cell. After the surface was modified with H_2N-Ph-NH_2 (GC-Ph-NH_2), the electrodes were rinsed with copious amounts of Milli-Q water, CH_3CN, and Milli-Q water and finally dried under a stream of nitrogen gas.

The GC-Ph-NH_2 surface was immersed in a solution containing 5 mM $NaNO_2$ and 0.5 M HCl for 20 min, followed by cycling between 0.6 and −0.8 V *versus* Ag/AgCl in a solution of AuNPs for five cycles at a scan rate of 100 mV s^{-1} to form the GC-Ph-AuNP electrode.

The GC-Ph-AuNP electrode was then immersed in a solution of anti-CEA (200 μg mL^{-1} in 0.1 M phosphate buffer (PB), pH 7.3) for 6 h at 4 °C to absorb the antibodies. Finally, the modified immunosensor was incubated in a solution of BSA (10 mg mL^{-1}) for about 1 h at room temperature. The immunosensor was stored at 4 °C when not in use.

CEA could be immobilized on the anti-CEA-modified GC electrode surface because of the strong affinity between CEA and anti-CEA. Electrochemistry was used to monitor the attachment of each component.

3. Results and discussion

3.1. Fabrication principles of the immunosensor

The long-term stability of the interface based on AuNPs is required for its practical application, particularly as a biosensor. The most common methods to immobilize AuNPs are based on the affinity between thiol groups and gold to form S—Au bonds or between amines and gold to form NH—Au bonds. The bond energy for a S—Au bond is 1.6 eV, corresponding to 154.4 kJ mol^{-1} (Ramachandran et al., 2003; Gronbeck et al., 2000). The bond energy for a NH—Au bond is 1.59 eV, which corresponds to a NH—Au bond strength of 153.6 kJ mol^{-1} (Fagas and Greer, 2007). It has been proposed that the stability can be improved through the formation of C—Au bond, which has a bond energy of 3.29 eV, corresponding to 317.1 kJ mol^{-1} (Partyka et al., 2006). This bond energy is significantly greater than those of S—Au and NH—Au bonds. As a result, a novel CEA immunosensor was designed based on the properties of C—Au bonds (Scheme 1).

3.2. Optimization of the size of the AuNPs for the immunosensor

Because the size of AuNPs has influence on the capability of electron transfer between the electrode and AuNPs, and on the stability of the AuNPs immobilized on the electrode, different sizes of AuNPs should be optimized. The AuNPs with 5, 10, 15, 20, 40, and 65 nm in diameter were used to fabricate the GC-Ph-AuNP electrode. The stability of the electrode containing AuNPs with different sizes was conducted by calculating the decrease of the

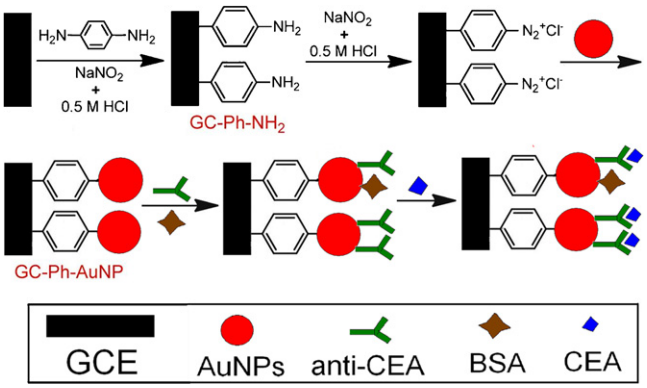

Scheme 1. Preparation of the GC-Ph-AuNP immunosensor and competitive immune reaction.

amount of the AuNPs after the sonication of electrodes in Milli-Q water for 3 min. The amount of AuNPs on GC-Ph-AuNP electrode was calculated according to a literature (Hoogvliet et al., 2000). The GC-Ph-AuNP electrode fabricated by 40 and 65 nm AuNPs lost *ca.* 5% and 8% AuNPs after sonication, respectively. While the AuNPs modified on the electrode with 5, 10, 15, 20 nm remained almost the same before and after sonication. To address the effect of the size of the AuNPs on the capability of electron transfer, the performance of the GC-Ph-AuNP electrode fabricated by 5, 10, 15, and 20 nm AuNPs was studied with CV in PBS-$[Fe(CN)_6]^{4-/3-}$ (Fig. S1). The data indicated that the immunosensors fabricated by the AuNPs with 20 nm in diameter have a better capability of the electron transfer. Considering to the stability and the conductivity, the 20 nm AuNPs was used to fabricate the immunosensor.

3.3. Fabrication and characteristics of the electrochemical immunosensor

A GC electrode surface was first modified with H_2N-Ph-NH_2 (GC-Ph-NH_2). The selective diazotization of one amine group of H_2N-Ph-NH_2 was achieved by the addition of 1 eq. of $NaNO_2$ to 1 eq. of H_2N-Ph-NH_2 dissolved in HCl solution. The resulting aminophenyl diazonium cations were used to directly graft aminophenyl groups onto the surface of the GC electrode (Lyskawa and Belanger, 2006). Then, the terminal amine groups were converted to diazonium groups by incubating the GC-Ph-NH_2 interface in a solution of $NaNO_2$ and HCl to form GC-Ph-$N_2^+Cl^-$. AuNPs were then immobilized on the interface *in situ* by scanning CV to give a 4-phenyl-AuNP-modified interface (GC-Ph-AuNP). Tethering AuNPs to the electrode surface by C—Au bonds could increase the stability of the AuNP layer. Anti-CEA was directly adsorbed on the AuNPs fixed on the GC electrode. The modified immunosensor was incubated in BSA solution to block any possible remaining active sites on the AuNPs. The stable GC-Ph-AuNP immunosensor was fabricated to detect CEA.

The modification of the GC electrode was monitored by CV in 10 mM $[Fe(CN)_6]^{4-/3-}$(contains 0.1 M KCl) at 50 mV s^{-1} (Fig. 1A). A redox peak of $[Fe(CN)_6]^{4-}$ was observed for the bare GC electrode (curve a). The redox peak current decreased when the GC electrode was modified with H_2N-Ph-NH_2 (curve b) because the formation of C—C bonds impeded the transfer of electrons between the electrode surface and electrolyte. The redox peak current decreased after the GC electrode was modified with AuNPs (curve c) because of the repulsion between the negatively charged AuNPs and $[Fe(CN)_6]^{4-}$ (An et al., 2007). The redox peak current decreased again after anti-CEA was immobilized on the GC electrode (curve d) due to the formation of an electron-blocking layer. The AuNPs and GC-Ph-AuNP electrode were characterized by TEM (Fig. S2) and AFM (Fig. S3), respectively, as shown in Supplementary information.

3.4. Stability of the electrochemical immunosensor

The stability of the GC-Ph-AuNP immunosensor was determined by comparison with GC-Ph-NH-AuNP (Scheme S1A) and GC/NH-Ph-NH-AuNP (Scheme S1B) immunosensors. The fabrication methods of the latter two immunosensors are shown in Supplementary information. The relative currents of the GC-Ph-AuNP, GC-Ph-NH-AuNP, and GC/NH-Ph-NH-AuNP immunosensors following incubation at pH 7.0 in PB at 4 °C are displayed in Fig. 1B. The relative current of each freshly fabricated immunosensor is considered to be 1. The currents increased by 4, 8, and 14%, for the GC-Ph-AuNP (dot a), GC-Ph-NH-AuNP (dot b), and GC/NH-Ph-NH-AuNP (dot c) immunosensors, respectively, after 30 days. This shows that the GC-Ph-AuNP immunosensor was much more stable than the GC-Ph-NH-AuNP and GC/NH-Ph-NH-AuNP immunosensors.

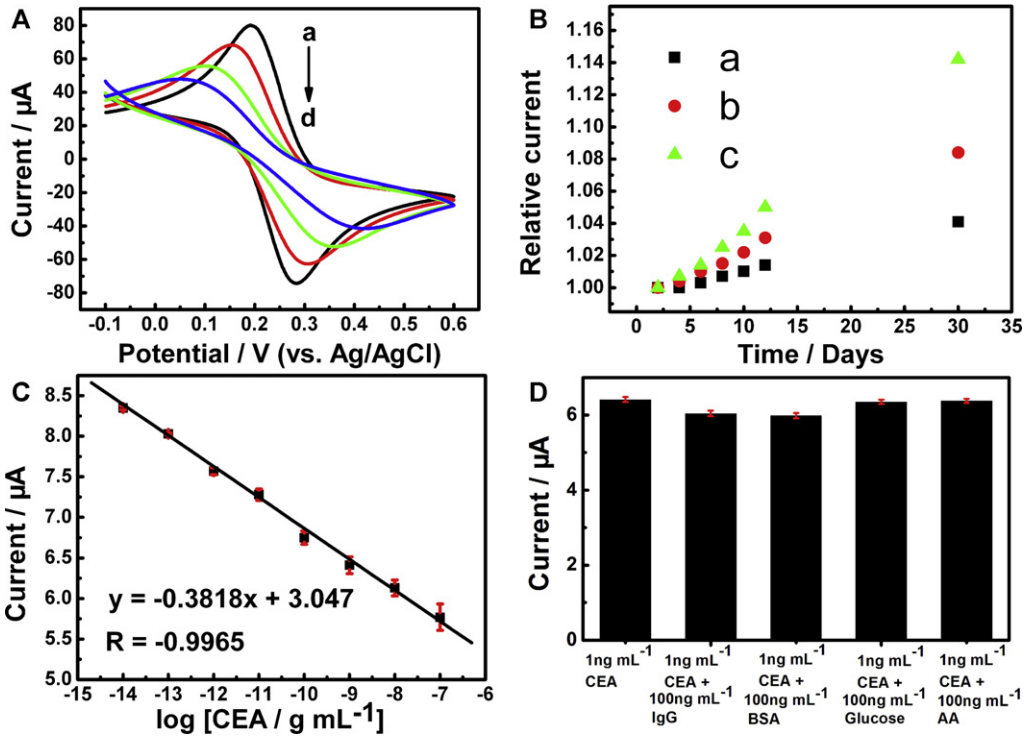

Fig. 1. (A) Cyclic voltammograms of modify procedure in 10 mM $[Fe(CN)_6]^{4-/3-}$(containing 0.1 M KCl) solution; (B) the relative current of DPV of three immunosensors with anti-CEA and without CEA following the different incubation time in pH 7.0 PBS at 4 °C for triplicates. (C) Calibration polt of current against log CEA concentration for the immunosensor under the optimization conditions; (D) amperometric response of the immunosensor to 1 ng mL^{-1} CEA, 1 ng mL^{-1} CEA + 100 ng mL^{-1} IgG, 1 ng mL^{-1} CEA + 100 ng mL^{-1} BSA, 1 ng mL^{-1} CEA + 100 ng mL^{-1} Glucose and 1 ng mL^{-1} CEA + 100 ng mL^{-1} AA.

Table 1
The properties of this sensor compared with others reported.

Sensors	Immobilize method of AuNPs	Linear response range ($ng\,mL^{-1}$)	Detection limit ($ng\,mL^{-1}$)	Refs.
Anti-CEA/AuNP@nafion/FC@CHIT/GCE	Block copolymer matrixes	0.01–150	0.003	Shi and Ma (2011)
HRP-Anti-CEA/nanogold/DNA/Au electrode	Electrostatic interactions	0.5–300	0.1	Tang et al. (2006)
Anti-CEA/Au_4-CTS_4/GCE	Electrostatic interactions	0.5–80	0.27	Fu et al. (2006)
Anti-CEA/nano-Au particle/Au/Fe_3O_4 nanoparticle/SPCE	S—Au bond, NH—Au bond	0.005–50	0.001	Li et al. (2010)
Anti-CEA/GNP-Thi-GR/GCE	S—Au bond, NH—Au bond	0.01–0.5	0.004	Kong et al. (2011)
Anti-CEA/Au-Ph-GCE	C—Au bond	0.00001–100	0.000003	This work

3.5. Performance of the immunosensor

To assess the dynamic working range of the GC-Ph-AuNP immunosensor, CEA was detected in pH 7.0 PBS-$[Fe(CN)_6]^{4-/3-}$ solution by DPV. The DPV peak current decreased with the incremental CEA concentration (Fig. 1C). The curve in Fig. 1C shows that the decrease of anodic current was proportional to CEA concentration in the range of 10 fg to 100 ng mL^{-1}, and the linear regression equation is i_{pc} (μA) = $-0.3818 \times \log C$[CEA] + 3.047 ($g\,mL^{-1}$) (R^2 = 0.993) with a LOD of 3 fg mL^{-1} (S/N = 3). The standard deviation of the detection limits is 0.23 fg.

To characterize the specificity of the immunosensor, 1 ng mL^{-1} of CEA was mixed with 100 ng mL^{-1} of IgG, BSA, glucose, and AA, respectively, and then the immunosensor response was measured. Compared with the amperometric response obtained from pure CEA, the variation in current caused by the interference substances was less than 6% (Fig. 1D), indicating that the immunosensor possesses good selectivity for CEA. To further address the selectivity of the present immunosensor, the control experiment incubating sensor with a mixture of IgG, BSA, glucose, and AA but without CEA was conducted. For the addition of 1 ng mL^{-1} CEA, current decrease is 3.38 μA. In contrast, the current decrease is only 0.44 μA for adding the mixture containing 100 ng mL^{-1} glucose, 100 ng mL^{-1} AA, 100 ng mL^{-1} BSA, and 100 ng mL^{-1} IgG. This result showed that the present immunosensor has a good selectivity (as shown in Fig. S4 in Supplementary information).

The performance of the GC-Ph-AuNP immunosensor was examined; its LDR and LOD (S/N = 3) are listed in Table 1. The LOD and LDR of this immunosensor are superior to those of other immunosensors using electrostatic interactions, block copolymer matrices, S—Au bonds, and NH—Au bonds to immobilize AuNPs (Tang et al., 2006; Kong et al., 2011; Li et al., 2010; Fu et al., 2006; Shi and Ma, 2011). For the LOD and LDR of immunosensor associating with electron transfer between electrode and AuNPs, the effect of the differences among C—Au (formation by directly connecting benzyl group to AuNPs), S—Au, and N—Au bonds on the promoting electron transfer between electrode and AuNPs was studied. The GC-Ph-AuNP, GC-Ph-NH-AuNP, GC-Ph-S-AuNP, and GC/NH-Ph-NH-AuNP electrodes were prepared and their CVs were also measured (Fig. S5A). The fabrication methods of those four electrodes were shown in Supplementary information. The CV results indicated that the GC-Ph-AuNP electrode is most conductive than those of the other electrodes, showing that the formation of C—Au bond by directly connecting benzyl group to AuNPs is more beneficial to the electron transfer. Those caused the better performance for the present immunosensor. To further clarify it, the GC-Ph-NH-AuNP immunosensor was used to detect CEA. The linear range of the immunosensor was 100 fg to 1 ng mL^{-1} (as shown in Fig. S5B).

4. Conclusions

A stable electrochemical immunosensor based on AuNPs immobilized by C—Au bonds was fabricated to detect CEA. The current of the immunosensor increased by *ca.* 4% after one month, revealing that the method used to modify the AuNPs improved the stability of the immunosensor. The immunosensor exhibited a linear response to CEA concentration from 10 pg mL^{-1} to 100 ng mL^{-1} with a LOD of 3 fg mL^{-1} (S/N = 3). The immunosensor is simple, had a wide linear range, high selectivity, low LOD, and good stability. This immobilization method using C—Au bonds can be widely applied to construct other immunosensors.

Acknowledgments

This study was supported by Funding Project for Academic Human Resources Development in Institutions of Higher Learning under the Jurisdiction of Beijing Municipality (PHR20100718) and Development Program of Science and Technology of Beijing Municipal Education Commission (KM200810028010)

Appendix A. Supplementary data

Supplementary data associated with this article can be found, in the online version, at doi:10.1016/j.bios.2012.02.061.

References

An, H.Z., Yuan, R., Tang, D.P., Chai, Y.Q., Li, N., 2007. Electroanalysis 19, 479–486.
Bi, S., Zhou, H., Zhang, S., 2009. Biosens. Bioelectron. 24, 2961–2966.
Bosker, W., Huestis, M., 2009. Clin. Chem. 55, 1910–1931.
Centi, S., Laschi, S., Mascini, M., 2007. Talanta 73, 394–399.
Chen, H., Jiang, C., Yu, C., Zhang, S., Liu, B., Kong, J., 2009. Biosens. Bioelectron. 24, 3399–3411.
Coyle, V., Johnston, P., 2010. Nat. Rev. Clin. Oncol. 7, 90–97.
Dai, Z., Yang, Y., Wu, H., 2011. Biosens. Bioelectron. 28, 421–427.
Dutsch-Wicherek, M., 2010. Am. J. Reprod. Immunol. 63, 181–188.
Fagas, G., Greer, J.G., 2007. Nanotechnology 18, 1–4.
Frens, G., 1973. Nature 241, 20–22.
Fu, Y.Z., Yuan, R., Chai, Y.Q., Zhang, Y., Peng, Y.G., 2006. Electroanalysis 18, 2451–2457.
Gas, F., Baus, B., Pinto, L., Compere, C., Tanchou, V., Quemeneur, E., 2010. Biosens. Bioelectron. 25, 1235–1239.
Gronbeck, H., Curioni, A., Andreoni, W., 2000. J. Am. Chem. Soc. 122, 3839–3842.
Gunaseelan, S., Gunaseelan, K., Deshmukh, M., Zhang, X., Sinko, P., 2010. Adv. Drug Deliv. Rev. 62, 518–531.
Haryono, A., Binder, W.H., 2006. Small 2, 600–611.
Hoogvliet, J.C., Dijksma, M., Kamp, B., van Bennekom, W.P., 2000. Anal. Chem. 72, 2016–2021.
Kong, F.Y., Xu, M.T., Xu, J.J., Chen, H.Y., 2011. Talanta 85, 2620–2625.
Leibowitz, F.L., Zheng, W., Maye, M.M., Zhong, C.-J., 1999. Anal. Chem. 71, 5076.
Lefkowitz, R., Marciniak, J., Hu, C., Schmid-Schonbein, G., Heller, M., 2010. Electrophoresis 31, 403–410.
Li, H.Q., Wang, C.G., Ma, Z.F., Su, Z.M., 2006. Anal. Bioanal. Chem. 384, 1518–1524.
Li, J.P., Gao, H.L., Chen, Z.Q., Wei, X.P., Yang, C.F., 2010. Anal. Chim. Acta 665, 98–104.
Liu, Z., Liu, J., Shen, G., Yu, R., 2006. Electroanalysis 18, 1572–1577.
Lyskawa, J., Belanger, D., 2006. Chem. Mater. 18, 4755–4763.
Ma, Z.F., Sui, S.F., 2002. Angew. Chem. Int. Ed. 41, 2176–2179.
Ma, Z.F., Wu, J.L., Zhou, T.H., Chen, Z.H., Dong, Y.G., Tang, J.T., Sui, S.F., 2002. New J. Chem. 26, 1795–1798.
Malhotra, R., Patel, V., Vaqué, J.P., Gutkind, J.S., Rusling, J.F., 2010. Anal. Chem. 82, 3118–3123.
Pacifico, J., Gomez, D., Mulvaney, P., 2005. Adv. Mater. 17, 415–418.
Partyka, D.V., Zeller, M., Hunter, A.D., Gray, T.G., 2006. Angew. Chem. Int. Ed. 45, 8188–8191.
Ramachandran, G.K., Hopson, T.J., Rawlett, A.M., Nagahara, L.A., Primak, A., Lindsay, S.M., 2003. Science 300, 1413–1416.
Shenhar, R., Jeoung, E., Srivastava, S., Norsten, T.B., Rotello, V.M., 2005. Adv. Mater. 17, 2206–2210.
Shi, W.T., Ma, Z.F., 2011. Biosens. Bioelectron. 26, 3068–3071.
Song, C.Y., Wang, Z.Y., Zhang, R.H., 2009. Biosens. Bioelectron. 25, 826–831.

Su, L., Mao, L.Q., 2006. Talanta 70, 68–74.
Tang, D.Q., Zhang, D.J., Tang, D.Y., Ai, H., 2006. Electroanalysis 18, 2194–2201.
Tang, L.C., Dong, C., Ren, J., 2010. Talanta 81, 1560–1567.
Templeton, A.C., Zamborini, F.P., Wuelfing, W.P., Murray, R.W., 2000. Langmuir 16, 6682.
Tognarelli, D.J., Miller, R.B., Pompano, R.R., Loftus, A.F., Sheibley, D.J., Leopold, M.C., 2005. Langmuir 21, 11119–11127.
Wang, Y., Tang, Z.Y., Correa-Duarte, M.A., Liz-Marzan, L.M., Kotov, N.A., 2003. J. Am. Chem. Soc. 125, 2830–2831.
Wang, M.J., Wang, L.Y., Yuan, H., 2004a. Electroanalysis 16, 757–764.
Wang, C.G., Ma, Z.F., Wang, T.T., Su, Z.M., 2006a. Adv. Funct. Mater. 16, 1673–1678.
Wang, Z.P., Hu, J.Q., Jin, Y., 2006b. Clin. Chem. 52, 1958–1961.
Wang, C.G., Chen, Y., Wang, T.T., Ma, Z.F., Su, Z.M., 2007. Chem. Mater. 19, 5809–5811.
Wang, C.G., Chen, Y., Wang, T.T., Ma, Z.F., Su, Z.M., 2008. Adv. Funct. Mater. 18, 355–361.
Wang, M.J., Wang, L.Y., Wang, G., 2004b. Biosens. Bioelectron. 19, 575–582.
Wohltjen, H., Snow, A.W., 1998. Anal. Chem. 70, 2856.
Xu, H., Hong, R., Wang, X.Y., Arvizo, R., You, C.C., Samanta, B., Patra, D., Tuominen, M.T., Rotello, V.M., 2007. Adv. Mater. 19, 1383–1386.
Xu, S.J., Liu, Y., Wang, T.H., 2010. Anal. Chem. 82, 9566–9572.
Xu, S.J., Liu, Y., Wang, T.H., 2011. Anal. Chem. 83, 3817–3823.
Yamanoi, Y., Yonezawa, T., Shirahata, N., Nishihara, H., 2004. Langmuir 20, 1054–1056.
Zhang, J., Lei, J.P., Xu, C.L., Ding, L., Ju, H.X., 2010. Anal. Chem. 82, 1117–1122.